J. Am. Soc. Mass Spectrom. (2019) 30:2092–2100
DOI: 10.1007/s13361-019-02279-3

RESEARCH ARTICLE

Nitrogen-Activated Oxidation in Nitrogen Direct Analysis in Real Time Mass Spectrometry (DART-MS) and Rapid Detection of Explosives Using Thermal Desorption DART-MS

ShuQi An, Shuai Liu, Jie Cao, ShiFang Lu

Key Laboratory of Cluster Science, Ministry of Education of China; Beijing Key Laboratory of Photoelectronic/Electrophotonic Conversion Materials; School of Chemistry, Beijing Institute of Technology, Beijing, 100081, China

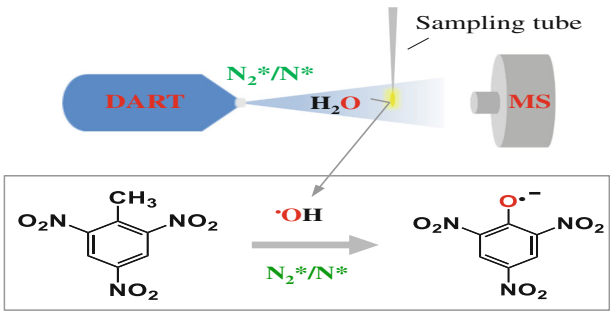

Abstract. Direct analysis in real time mass spectrometry (DART-MS) was used to analyze an array of explosives including nitro-based explosives, peroxide explosives, and energetic heterocyclic compounds with different DART discharge gases (helium, argon, and nitrogen). Profound analyte oxidation was observed for particular compounds (TNT (9) and 2, 4-DNT (10)), whose mass spectra were completely dominated by the oxidation products when nitrogen was substituted for helium in DART analysis. This interesting phenomenon suggested that a highly oxidative environment provided by N_2 DART ion source. A possible mechanism involved in nitrogen DART was proposed which may help further understanding the different chemistry involved in the ionization process. This work also presents a thermal desorption DART (TD-DART) configuration that can enable rapid, specific analysis of explosives from swipes. The screening of swipes with three different compositions (fiberglass, Hybond N^+ membrane, and filter paper) showed that fiberglass swipe has the best performance which was then used for the subsequent TD-DART analysis. A direct comparison of TD-DART with traditional DART demonstrated that TD-DART indeed gives better response than traditional DART (provided that the distance between the DART source and mass spectrometer is the same) and will have wider applications than traditional DART.

Keywords: Thermal desorption direct analysis in real time mass spectrometry (TD-DART-MS), Nitrogen-activated oxidation, Explosives

Received: 22 March 2019/Revised: 20 June 2019/Accepted: 25 June 2019/Published Online: 31 July 2019

Introduction

In recent years, explosive materials have been widely employed for various military applications and civilian conflicts; their use for hostile purposes has increased considerably. There is an ever-increasing need for rapid and specific identification of explosives to support forensic science and security applications. Mass spectrometry (MS) and ion mobility spectrometry (IMS) are effective tools to detect explosives [1–4]. IMS has been the conventional technique employed for these applications. Although rapid and reliable, there is an increasing interest in improving the specificity of IMS-based methods. Compared with IMS, MS technique has versatility and accuracy to identify the explosives being the most powerful tool for explosive investigations. Moreover, MS can be applied with different ionization methods such as electron ionization (EI)/chemical ionization (CI) [5–8], electrospray ionization (ESI) [9, 10], atmospheric pressure chemical ionization (APCI) [11, 12], desorption electrospray ionization (DESI) [13, 14], direct analysis in real time (DART) [15–18], and atmospheric pressure photoionization (APPI) [19]. Among all the ionization methods in MS, DART has demonstrated itself as one of the best methods to detect hundreds of chemicals including

Electronic supplementary material The online version of this article (https://doi.org/10.1007/s13361-019-02279-3) contains supplementary material, which is available to authorized users.

Correspondence to: Jie Cao; *e-mail:* jcao@bit.edu.cn

explosives due to the advantages of high-throughput, fast, and real-time analysis with minimal sample preparation.

DART is an ambient ionization method that is based on the interactions of excited-state atoms or molecules with analyte and atmospheric gases [15, 20]. Although this technique has been developed with noble gases as the most common DART gases, the ionization mechanism involved in nitrogen DART was not well understood. Nitrogen has a number of long-lived vibronic excited states, the maximum energy available for Penning ionization by N_2* is given as 11.5 eV [21]. The ionization energies (IE) of ambient gases, including nitrogen, water, oxygen, ammonia, and nitric oxide are 15.6, 12.6, 12.1, 10.0, and 9.3 eV, respectively [22]. Consequently, water cluster ions should not be present in the background mass spectra of N_2 DART. However, protonated water, O_2^+, and other reactive species can be observed in the background mass spectrum with nitrogen DART gas [23, 24], in which the formation mechanism of such species remains unclear.

Herein we present our systematic study of analysis of a series of explosives including nitro based explosives (i.e., TNT (9), RDX (11), and HMX (12)), peroxide explosives (i.e., HMTD (7) and TATP (8)), and energetic heterocyclic compounds (i.e., tetrazole-1, 5-diamine (1)) as a test case to probe the unique feature of N_2 DART with comparison to helium and argon DART in order to gain insights into the ionization mechanism of N_2 DART, which helps further understanding the chemistry involved in the ionization process. This work also shows that TD-DART can enable rapid and specific analysis of explosives from swipes. A direct comparison of TD-DART with traditional DART was made to compare the signal response for the same analyte.

Experimental

Materials and Sample Preparation

Methanol and acetonitrile (HPLC grade) were purchased from Sigma-Aldrich (St. Louis, MO, USA) and used for sample dilution. Compounds 1–6 and 9–10 were kindly provided by the State Key Laboratory of Explosion Science and Technology, Beijing Institute of Technology. Compounds 7–8 and 11–14 were purchased as solutions from AccuStandard Inc. (New Haven, CT, USA) at a concentration of 1 mg/mL or 0.1 mg/mL, in either methanol or acetonitrile, and further diluted in methanol as required. 1 mg mL^{-1} stock solutions of 1–6 in methanol and 9–10 in acetonitrile were prepared. Individual standards and standards mixtures were prepared by diluting the stock solutions with methanol to a final concentration. Fiberglass swipe, Hybond N^+ membrane, and filter paper were purchased from DSA Detection (North Andover, MA, USA), GE Healthcare Bioscience (Buckinghamshire, UK), and Whatman (Piscataway, NJ, USA), respectively. These membranes were cut into thin strips (with 10 × 5 mm in length × width) before use.

DART-MS Experiments

The mass spectrometric analysis was conducted with a DART ion source (IonSense, Saugus, MA, USA) coupled to Agilent 6520 Q-TOF mass spectrometer by a Vapur® hydrodynamic-assist interface (IonSense, Saugus, MA, USA). Unless otherwise noted, the distance from the DART source and the sampling orifice of Agilent 6520 Q-TOF is 1.0 cm. The DART source was operated with helium, argon, or nitrogen for analysis and nitrogen in the standby mode. Gas temperature was optimized to 350 °C (positive ion mode) and 300 °C (negative ion mode). Gas flow rate was set to 1.5 L min^{-1}. Grid electrode voltages were set to 250 V (positive ion mode) and − 250 V (negative ion mode), respectively. Mass spectra were acquired from *m/z* 50 to *m/z* 400. Vcap, 3500 V; skimmer, 65 V; OCT R_fV, 750 V; drying and nebulizer gas, N_2; nebulizer, 0 psi; drying gas flow, 1 L min^{-1}; drying gas temperature, 300 °C. Compounds 1–14 were measured under their optimal activator voltages (which is referred to the voltage applied between the sampling capillary and the skimmer in the ion optical module in front of the mass analyzer). Samples were analyzed by pipetting 2 μL of solutions onto the sealed end of melting tube, allowed to dry, and the tube was then suspended in the DART gas stream. For the membrane screening, 2 μL of sample solution was dropped onto different membrane, allowed to dry, and the membrane was then inserted in-between the DART source and mass spectrometer for analysis. All data were collected and processed using MassHunter (Agilent Technologies (China) Co., Ltd.) workstation software.

TD-DART-MS Experiments

The thermal desorber was configured between the DART and the entrance of mass spectrometer. Thermal desorption temperature up to 350 °C were controlled using an external temperature controller. Two microliter of sample solution was deposited onto the swabs. After evaporation of solvent, the swabs were inserted into the thermal desorber which was heated at various desorption temperatures. Heated vapors containing desorbed materials were orthogonally evacuated and drawn into the DART gas stream for ionization using a negative pressure system.

Results and Discussion

A total of 14 explosives (Figure 1), including 6 nitro explosives, 2 peroxide explosives, and 6 energetic heterocyclic compounds, were analyzed using DART ionization source in both positive-ion and negative-ion modes. First of all, the following important instrumental parameters were optimized in order to get the highest signal intensity. Figure 2 shows the distance effect on the signal intensity by plotting the absolute ion abundance of protonated molecule $[M + H]^+$ for compound 6 against L_1 (distance between DART source and sample) and L_2 (distance between DART source to the sampling orifice of mass spectrometer), respectively. It was found that the intensity

of protonated molecule $[M + H]^+$ tends to decrease first and then increase gradually with an increase of L_1 when fixing L_2 = 8 cm, showing dual maxima at L_1 = 0.5 cm and 7.0 cm, respectively (Figure 2a). This curvature indicates that sample needs to be close either to the ion source or to the mass analyzer (which can facilitate the ionization/thermal desorption of sample and the extraction of the ions to the mass spectrometer) in order to achieve the highest signal intensity. By keeping L_1 = 0.5 cm, the intensity of $[M + H]^+$ dramatically decreases as L_2 increases as expected (Figure 2b). Also, we use compounds 6 and 10 as examples to illustrate the impact of activator voltage on the signal intensity of molecular ions in the positive- and negative-ion mass spectra (Figure S1 in the supporting information). It can be clearly seen from Figure S1 that severe hydrated, protonated molecular ions $[M + H + nH_2O]^+$ ($n \geq 2$) as well as the protonated dimeric ion $[2\,M + H]^+$, indicating strong inter- and intramolecular hydrogen bonds formed between this type of molecule and water and within themselves, were found at low activator voltages and however, they are noticeably decreased with increase of activator voltage from 160 to 200 V for compound 6 (Figure S1a in the supporting information). For compound 10, the intensity of molecular anion $[M\text{-}H]^-$ increased with increasing the activator voltage from 80 to 160 V (not shown), but dropped down substantially when raising the voltage above 160 V accompanied with the fragment ion $[M–NO]^-$ jumping to be the base peak (Figure S1b in the supporting information).

Comparison of Mass Spectra Obtained by Ar--DART, He-DART, and N_2-DART

Next, we are going to explore the DART gas effect on the detection of explosives. Three working gases, helium (He), argon (Ar), and nitrogen (N_2) were used for the study. Helium is popularly used in DART-MS as it theoretically gives the best sensitivity. Although the DART ionization mechanisms are not yet fully understood, it was proposed that in the positive ion (PI) mode, metastable helium atoms (2^3S electronic excited state atoms with an internal energy of 19.8 eV) induce Penning ionization of ambient water in the open air, generating protonated water clusters, mostly $H_5O_2^+$, which further ionize analytes through chemical reactions [25]. In the negative ion (NI) mode, it was proposed that thermal electrons generated from the collision between electrons and gas molecules in the open air undergo electron capture by atmospheric oxygen to generate $O_2^{-\cdot}$, which further ionizes analytes through chemical reactions [16]. The molecular ions are usually present as $[M + H]^+$, $M^{+\bullet}$, $[M - H]^+$, and/or $[M + NH_4]^+$ in the PI mode and $M^{-\bullet}$ and $[M - H]^-$ in the NI mode. Helium has successfully been replaced by argon as the DART gas in order to provide softer ionization. However, the lower internal energy of metastable argon $^3P_2$ and $^3P_0$ states (11.55 and 11.72 eV, respectively) cannot ionize water, which in turn results in poor sensitivity. The application of dopant-assisted Ar-DART on the selective ionization of melamine [26], polycyclic aromatic hydrocarbons (PAHs) [27], and a variety of labile compounds such as nucleosides, alkaloids and glucoses [28] demonstrated that 1–2 orders of magnitude increase in detection signals. In this work, we also show the use of dopant (5% chlorobenzene) in the identification of 9 and 10 ($[M\text{-}H]^-$ at *m/z* 227 for 9 and *m/z* 182 for 10) can greatly increase the sensitivity by several times in Ar-DART (Figure S2 in the supporting information). Except for the sensitivity, Ar-DART mass spectra are identical with He-DART spectra for all compounds under study.

Nitrogen, inexpensive and readily available, has been only used as the DART discharge gas occasionally [23, 29–35] although the inventors of DART did suggest nitrogen as an alternative to helium and argon as the DART discharge gas, but little data was published to promote the application of N_2 DART. Cody et al. [15] indicated that N_2 DART primarily produces vibronically excited–state nitrogen molecules. Theoretically, N_2 DART should have lower ionization efficiency but less in source fragmentation than He DART because internal energies of metastable N_2 (three major metastable states $A^3\Sigma_u^+$ (6.16 eV), $E^3\Sigma_g^+$ (11.9 eV), and $a^1\Pi_g$ (8.5 eV) [21] are much lower than that of metastable helium atom. This was confirmed by our comparative study using three DART gases (Figures S3–S5 in the supporting information). Similar, but different—sensitivity DART mass spectra (helium, argon, and nitrogen) were obtained for the 12 explosives (not including 9 and 10), in which the dominating ions are $[M + H]^+$ and $[2\,M + H]^+$ for 1–6; $[M + H]^+$ and $[M + NH_4]^+$ for 7 and 8; $[M + NO_2]^-$, or $[M + NO_3]^-$ for 11–14, respectively.

More interestingly, the N_2 DART mass spectra of 9 and 10 showed noteworthy difference between N_2 DART and helium (and argon) DART (Figure 3), in which a range of oxidation products (trinitrophenol (TNP) and 2, 4-dinitro-6-hydroxybenzaldehyde for 9; dinitrophenol (DNP); and 2, 4-dinitrobenzoic acid for 10) are present, indicating that the molecular anions produced in the N_2 DART source were so vulnerable (they are completely absent in the corresponding spectra) that they readily underwent extensive oxidation reactions presumably triggered by trace oxidative species, i.e., hydroxyl radical which might be generated at the initial stage of ionization [23, 35]: $N_2^*/N^* + NH_3 \rightarrow N_2/N + NH_3^{+\bullet} + e^-$ (as $N_2^*/N^* > IE\ (NH_3)$); $NH_3^{+\bullet} + H_2O \rightarrow HO^\bullet + NH_4^+$ (as $PA\ (NH_3) > PA\ (HO^\bullet)$). The as-formed $HO^\bullet$ radicals participated in the oxidation of 9 and 10 through multiple steps to form the main oxidation products TNP and DNP [36], identified as $[TNP\text{-}H]^-$ (*m/z* 228, base peak) and $[DNP\text{-}H]^-$ (*m/z* 183, base peak), and further oxidation products (shown at *m/z* 211), respectively. The tandem mass spectra of the major oxidation products of 9 and 10 were given in the Figure S6 in the supporting information. It should be noted that the isomeric, further oxidation products at the same *m/z* 211 of 9 and 10 may have different structures, which were assigned as 2, 4-dinitro-6-hydroxybenzaldehyde for 9 and 2, 4-dinitrobenzoic acid for 10, respectively, based on the comparison of their spectra with those reported in the literature [36, 37]. These preliminary

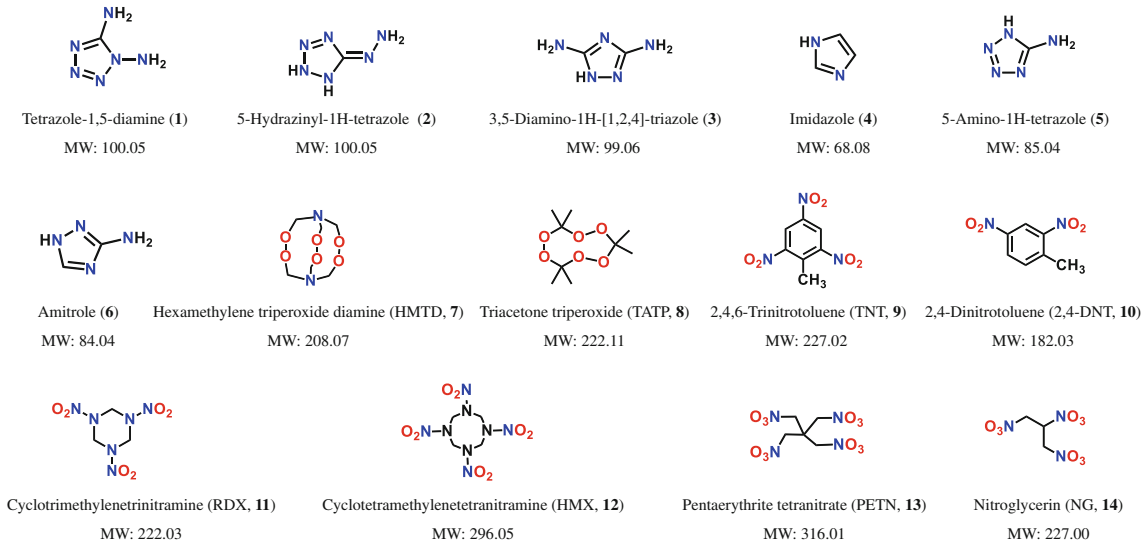

Figure 1. The structure of explosives under the study

results suggest that deprotonation by O_2^- may play a great role in the negative ion formation by nitrogen DART. The oxidation mechanisms of 9 and 10 were proposed in Figure 4, inspired by the oxidation mechanism of neutral 9 [38]. We also analyzed the analogous compounds of 9 and 10 (*i.e.*, nitrobenzene and *o*-, *p*-, *m*-nitrotoluene) by N_2 DART and surprisingly found out that (1) identical DART mass spectra with different gases (He, Ar, and N_2) were given (Figure S7 in the supporting information); (2) the change of detection ion polarity for negative to positive modes in nitrogen DART implied a different electron distribution of 9 and 10 from their analogues: the electron absorption of the nitro groups and their conjugation with benzene ring greatly reduces the electron density around the benzene ring and thus making the attached methyl group in 9 and 10 weakly acidic. Except for the abovementioned major ions in the N_2 DART spectra of 9 and 10, some common ions, i.e., $[M\text{-}NO]^-$ (*m/z* 197.0191) for 9; $[M + O\text{-}H]^-$ (*m/z* 197.0229), $[M\text{-}CH_3]^-$ (*m/z* 167.0102) for 10, were observed in the N_2, helium, and argon DART mass spectra. It was speculated that the complexity of N_2 DART mass spectra arising from complex oxidation reactions for some molecules could be the reason that restricts N_2 DART from wide applications.

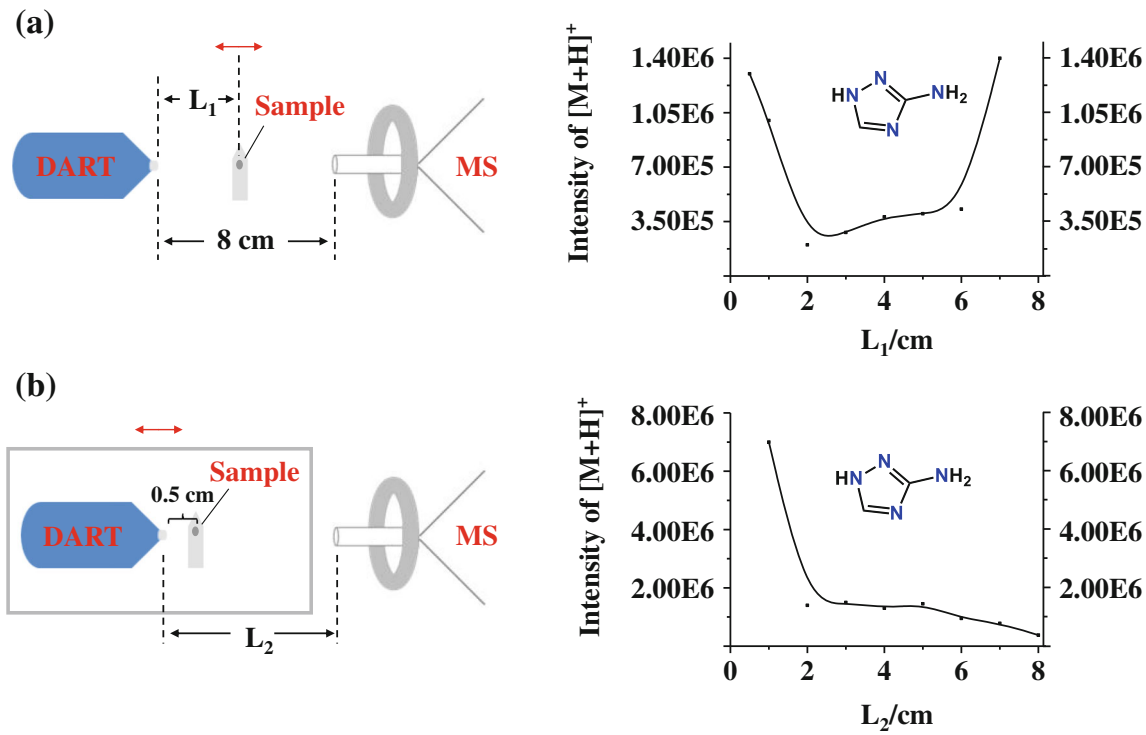

Figure 2. The effect of distances, (**a**) L_1 (from sample to the DART source) and (**b**) L_2 (from the DART source to the sampling orifice of mass spectrometer), on the absolute intensity of $[M + H]^+$ for compound 6 at a concentration of 50 ppm

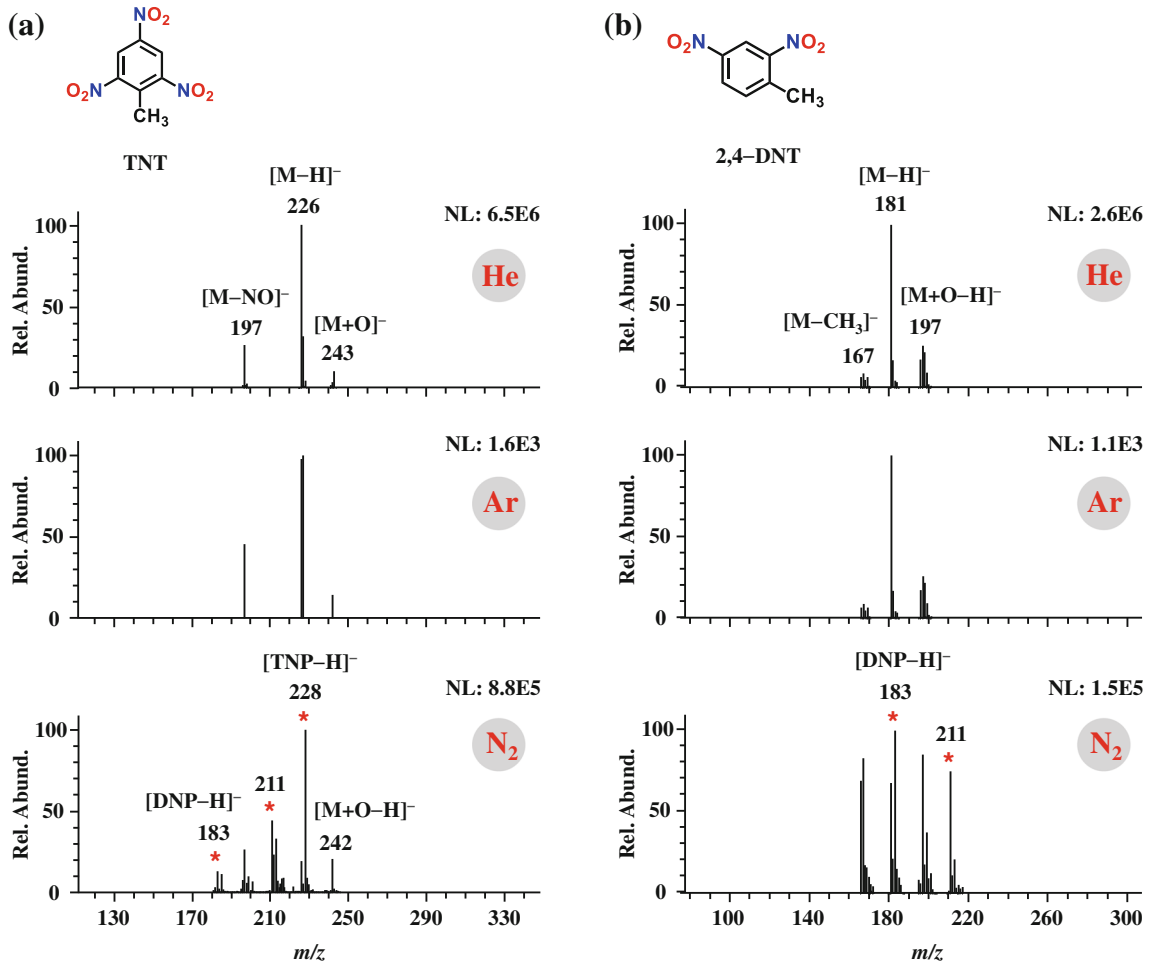

Figure 3. The negative-ion helium, argon and nitrogen DART mass spectra of (**a**) TNT and (**b**) 2, 4-DNT. The concentrations of analytes were 100 ppm in helium DART and nitrogen DART and 1000 ppm in argon DART, respectively. The highest peak in each mass spectrum is normalized to 100%, and the normalization level (NL) is indicated in the spectra

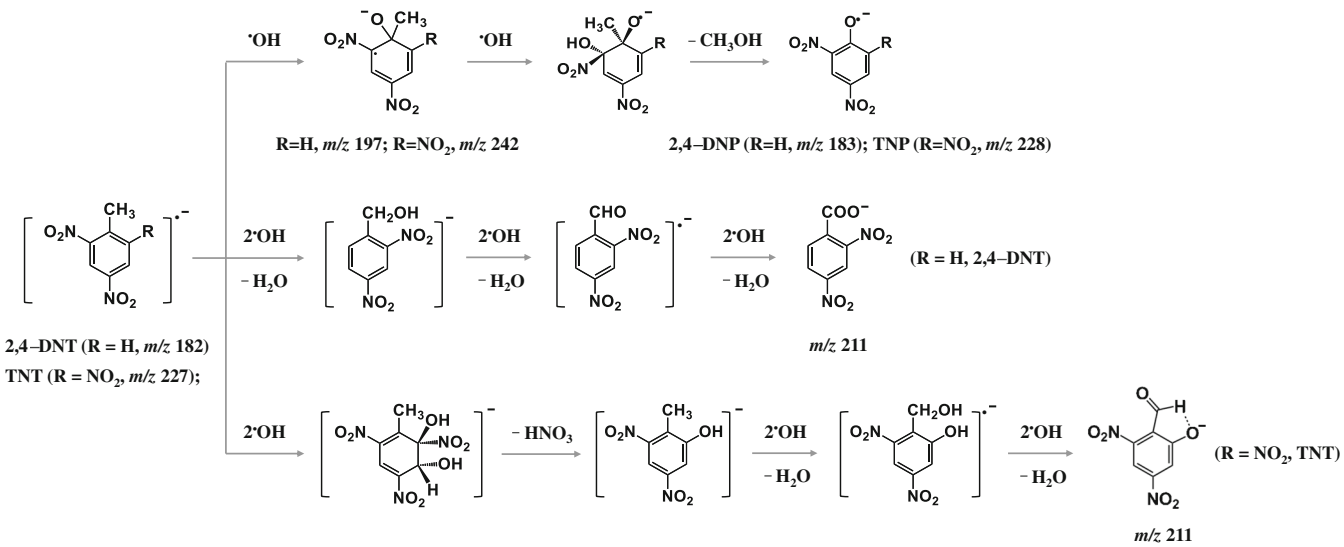

Figure 4. The proposed oxidation mechanism of TNT and 2, 4-DNT occurred in the N_2 DART

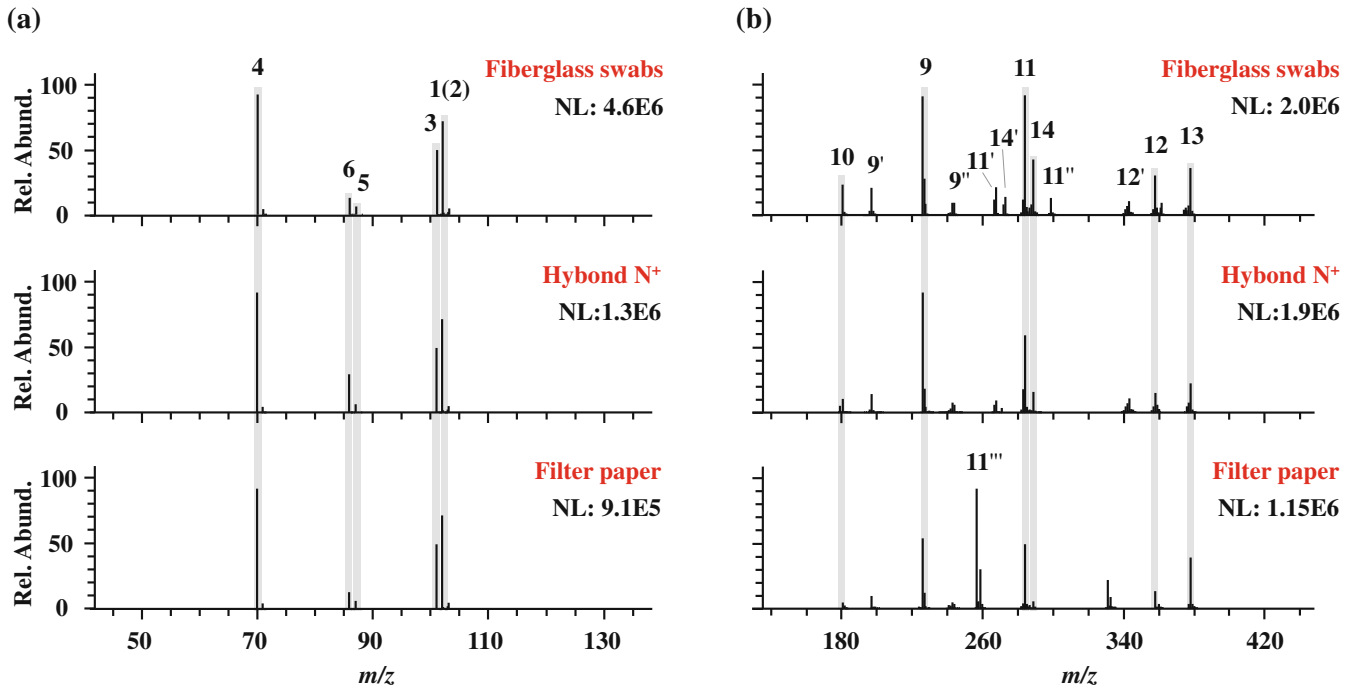

Explosives	Typical adducts or fragments (*m/z*)	Explosives	Typical adducts or fragments (*m/z*)	Explosives	Typical adducts or fragments (*m/z*)
1(2)	$[M+H]^+$ (101.0571)	**9**	$[M-H]^-$ (226.0113) **9** $[M-NO]^-$ (197.0227) **9'** $[M+O]^-$ (243.0118) **9''**	**12**	$[M+NO_3]^-$ (358.0336) **12** $[M+NO_2]^-$ (342.0394) **12'**
3	$[M+H]^+$ (100.0621)				
4	$[M+H]^+$ (69.0449)	**10**	$[M-H]^-$ (181.0247)	**13**	$[M+NO_3]^-$ (378.0017)
5	$[M+H]^+$ (86.0461)				
6	$[M+H]^+$ (85.0511)	**11**	$[M+NO_3]^-$ (284.0227) **11** $[M+NO_2]^-$ (268.0278) **11'** $[M+HCO_4]^-$ (299.0224) **11''** $[M+Cl]^-$ (257.0043) **11'''**	**14**	$[M+NO_3]^-$ (288.9904) **14** $[M+NO_2]^-$ (272.9944) **14'**
7	-				
8	-				

Figure 5. Comparison of helium DART mass spectra of mixtures consisting of 14 explosives in (**a**) positive and (**b**) negative modes using sampling swipes of different composition (fiberglass, Hybond N^+ membrane and filter paper). Typical adducts or fragments of each identifiable explosive were listed in the lower part of the figure. Note that multiple peaks were assigned to a single compound for some cases, i.e., 9, 9' and 9" were three abundant ions ($[M-H]^-$, $[M-NO]^-$, and $[M + O]^-$) belonging to TNT, respectively

Rapid Detection of Explosives Using TD-DART and a Comparative Study Using Traditional DART and TD-DART

There are limitations for the conventional DART configuration, one is the ionization/desorption efficiency is unknown and uncontrolled; the other is the traditional ways of sampling are impractical for rapid and selective analysis. There are several ways to enhance desorption/ionization efficiency so that stronger signals could be acquired. Laser can definitely help to improve the desorption efficiency. Liu et al [39] has utilized three-wavelength laser (IR, visible, and UV laser) in the novel plasma assisted multiwavelength (1064, 532, and 355 nm) laser desorption ionization mass spectrometry (PAMLDI-MS) system to provide broad possibilities for the compound desorption from the TLC plate used for mixture separation. The experimental results clearly showed that the introduction of laser has greatly improved the sensitivity and spatial resolution of the existing DART-MS method in which only a plasma-based ionization technique is involved. Heating is another cost-effective choice to facilitate the desorption process. Xu et al [40] reported an aerodynamic-assisted thermo desorption mass spectrometry method developed for the direct quantitative analyses of explosives from a distance. Sisco et al [41] used a thermal desorption direct analysis in real time mass spectrometry (TD-DART-MS) configuration for the detection and quantification of trace narcotic samples of a swipe material, which allows for desorption of the sample into a confined tube, completely independent of the DART source, allowing for more efficient and thermally precise analysis of material

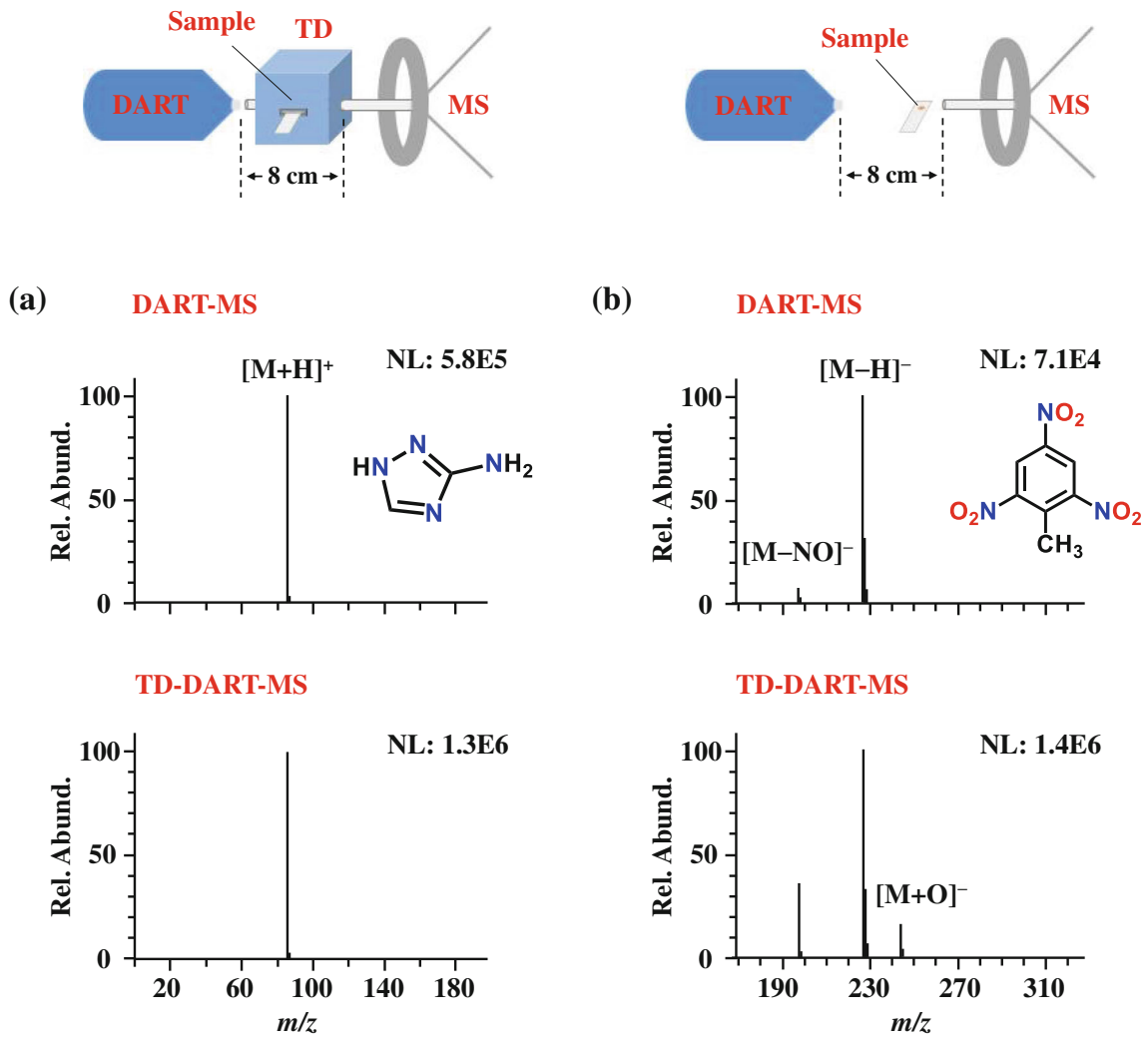

Figure 6. Comparison of TD-DART and conventional DART mass spectra of compounds (**a**) 6 and (**b**) 9 at a concentration of 50 ppm using PTFE-coated fiberglass swabs with keeping the distance of L_2 exactly the same (8 cm). Helium was used as DART gas for the measurements

present on a swipe. Thank Dr. Brian Musselman (Ion Sense, USA) and Dr. Charles Liu (ASPEC Technologies Limited, China) for providing us a newly invented thermal desorber coupled with traditional DART using sampling swipes, which enables rapid detection of explosives from swipes.

Swipe screening was first conducted in order to choose the one with the best performance for the subsequent TD-DART analysis. Mixture of explosives, comprising of eight (compounds 1–8) and six components (compounds 9–14), were prepared for the screening purpose. Three sampling swipes with different composition (fiberglass, Hybond N^+ membrane and filter paper) were used and the corresponding mass spectra were shown in Figure 5. It can be clearly seen from Figure 5 that fiberglass swipe gives the highest ion intensity for all explosives in both positive and negative modes, and the identifiable ions are almost the same for these swipes. The typical adducts or fragments of 14 explosives were listed in the lower part of Figure 5. Compounds 1–6 were identified mainly as $[M + H]^+$ on different swipes (Figure 5a). Note that the reason as to why 7 and 8 can be detected in the pure phase but not in the mixture is that their ionization efficiencies are the least competitive in the mixture because the proton affinity of oxygen atom (PA(O)) is far less than that of nitrogen atom (PA(N)).Compounds 9–14 in the second mixture were all detected, and the corresponding spectra were shown in Figure 5b. It should be noted that multiple peaks were assigned to a single compound in some cases (i.e., compounds 9, 11, 12, and 14) because they are all prominent in the respective spectra either as adducts or as fragment ions. For example, 9 has three labeled peaks (9, 9', and 9") at *m/z* 197, 226, and 243 which were assigned as $[M\text{-}NO]^-$, $[M\text{-}H]^-$, and $[M + O]^-$, respectively. Similarly, compound 11 was detected as four adducts corresponding to $[M + NO_3]^-$ (peak 11, *m/z* 284), $[M + NO_2]^-$ (peak 11' at *m/z* 268), $[M + HCO_4]^-$ (peak 11" at *m/z* 299), and $[M + Cl]^-$ (peak 11"' at *m/z* 257), respectively. The same situation happens for the other two compounds 12 and 14. Two types of molecular adduct ions ($[M + NO_3]^-$ (peak 12 at *m/z* 358 for 12; peak 14 at *m/z* 289 for 14) and $[M + NO_2]^-$ (peak 12' at *m/z* 342

for 12; peak 14' at *m/z* 273 for 14) were the dominant species in the respective spectra. Then, we utilize scanning electron microscope (SEM) and Fourier transform infrared spectroscopy (FT-IR) (Figure S8 in the supporting information) to characterize the composition and surface morphology of swipes in order to find out the reason to cause the different signal response of analytes. The results of FT-IR confirm the main component of fiberglass, Hybond N^+ membrane and filter paper are polytetrafluoroethylene (PTFE), polyamide, and cellulose, respectively, based on the characteristic peaks for each material, i.e., C-F symmetric and asymmetric stretching bands at 1150 cm^{-1} and 1240 cm^{-1} for fiberglass swipe [42]; amide I and II stretching bands at 1640 cm^{-1} and 3300 cm^{-1} (broad) for Hybond N^+ membrane [43, 44]; and the stretching vibrations of –OH at 3320 cm^{-1} (broad), methylene C–H at 2930 cm^{-1}, and C–O at 1020 cm^{-1} for filter paper [45, 46]. It is obvious that it is the surface morphology, not the surface composition, which contributes to the different ion intensity on different membranes. Filter paper has the roughest surface and the largest pore size compared with the other two membranes, which are unfavorable for efficient thermal desorption, and hence resulting in the lowest ion intensity.

A comparative study of TD-DART and conventional DART with PTFE-coated fiberglass swabs was performed, and the representative mass spectra were given in Figure 6 exemplified by compounds 6 and 10, respectively. It can be seen from Figure 6 that the intensity of protonated molecular ion $[M + H]^+$ for TD-DART is stronger than that for DART in both cases, suggesting that better signal response was indeed achieved in TD-DART than DART itself provided that the distance between the DART source and mass spectrometer is the same. Figures S9–10 in the supporting information were the TD-DART and DART mass spectra of 14 explosives at their optimal distances (where L_2 = 8 cm and 1 cm for TD-DART and DART, respectively). Similar spectra were obtained by DART and TD-DART. The "apparent" attenuation of the signal intensity in TD-DART is due to much longer distance of L_2 (8 cm vs. 1 cm for TD-DART vs. DART) being applied for TD-DART.

Conclusion

A total of 14 explosives were systematically analyzed using DART with three different DART discharge gases (helium, argon, and nitrogen) and TD-DART with helium. Profound analyte oxidation was observed for particular compounds (9 and 10), whose mass spectra were completely dominated by the oxidation products (e.g., trinitrophenol (TNP) for 9 and dinitrophenol (DNP) for 10) when nitrogen was substituted for helium in DART analysis. This interesting phenomenon suggested that a highly oxidative environment provided by N_2 DART ion source. A possible oxidation mechanism involved in nitrogen DART was proposed to account for the production of the oxidation products for 9 and 10, in which the hydroxyl radicals generated by nitrogen activation of water molecules play an important role in the entire oxidation process, and they can oxidize the organic substrate to form the oxidation products through multiple reaction steps. TD-DART was firstly utilized to analyze the explosives systematically with helium gas. A comparative study of TD-DART and traditional DART with swipes demonstrated that TD-DART indeed gives better response than traditional DART provided that the distance between the DART source and mass spectrometer is the same.

Acknowledgements

The authors thank (1) Dr. Brian Musselman (Ion Sense, USA) and Dr. Charles Liu (ASPEC Technologies Limited, China) for providing the newly invented, commercial TD-DART; (2) Robert B. Cody for his insightful discussions; (3) the technical supports from Dr. Xiaokun Duan (ASPEC) and Dr. Fred Li (Ion Sense); and (4) the analysis and testing center of Beijing Institute of Technology (BIT) at Liangxiang campus for providing the MS instrument for DART analysis. The authors also thank the National Natural Science Foundation of China (21371025), the 111 Project (B07012), and the Fundamental Research Grant (20121942006) by BIT.

References

1. Mäkinen, M., Nousiainen, M., Sillanpää, M.: Ion spectrometric detection technologies for ultra-traces of explosives: a review. Mass Spectrom. Rev. **30**, 940–973 (2011)
2. Pavlovich, M.J., Musselman, B., Hall, A.B.: Direct analysis in real time-mass spectrometry (DART-MS) in forensic and security applications. Mass Spectrom. Rev. **37**, 171–187 (2018)
3. Gross, J.H.: Direct analysis in real time-a critical review on DART-MS. Anal. Bioanal. Chem. **406**, 63–80 (2014)
4. Chernetsova, E.S., Morlock, G.E., Revelsky, I.A.: DART mass spectrometry and its applications in chemical analysis. Russ. Chem. Rev. **80**, 235–255 (2011)
5. Bulusu, S., Axenrod, T., Milne, G.W.A.: Electron-impact fragmentation of some secondary aliphatic nitramines. migration of the nitro group in heterocyclic nitramines. Org. Mass Spectrom. **3**, 13–21 (1970)
6. Meyerson, S., Haar, R.W.V.: Organic ions in gas phase. XXVI. decomposition of 1,3,5-trinitrobenzene under electron impact. J. Organomet. Chem. **37**, 4114–4119 (1972)
7. Burrows, E.P.: Dimethyl ether and dimethyl-d_6 ether chemical ionization mass spectrometry of nitramines, nitroaromatics and related compounds. Org. Mass Spectrom. **29**, 315–320 (1994)
8. Zitrin, S.: The chemical ionization mass spectrometry of RDX. Org. Mass Spectrom. **17**, 74–78 (1982)
9. Wu, Z.G., Hendrickson, C.L., Rodgers, R.P., Marshall, A.G.: Composition of explosives by electrospray ionization fourier transform ion cyclotron resonance mass spectrometry. Anal. Chem. **74**, 1879–1883 (2002)
10. Straub, R.F., Voyksner, R.D.: Negative ion formation in electrospray mass spectrometry. J. Am. Soc. Mass Spectrom. **4**, 578–587 (1993)
11. Popov, I.A., Chen, H., Kharybin, O.N., Nikolaev, E.N., Cooks, R.G.: Detection of explosives on solid surfaces by thermal desorption and ambient ion/molecule reactions. Chem. Commun. 1953–1955 (2005)
12. Song, Y.S., Cooks, R.G.: Atmospheric pressure ion/molecule reactions for the selective detection of nitroaromatic explosives using acetonitrile and air as reagents. Rapid Commun. Mass Spectrom. **20**, 3130–3138 (2006)
13. Cotte-Rodríguez, I., Takáts, Z., Talaty, N., Chen, H.W., Cooks, R.G.: Desorption electrospray ionization of explosives on surfaces: sensitivity and selectivity enhancement by reactive desorption electrospray ionization. Anal. Chem. **77**, 6755–6764 (2005)

14. Takáts, Z., Cotte-Rodríguez, I., Talaty, N., Chen, H.W., Cooks, R.G.: Direct, trace level detection of explosives on ambient surfaces by desorption electrospray ionization mass spectrometry. Chem. Commun. 1950–1952 (2005)
15. Cody, R.B., Laramée, J.A., Durst, H.D.: Versatile new ion source for the analysis of materials in open air under ambient conditions. Anal. Chem. **77**, 2297–2302 (2005)
16. Song, L.G., Dykstra, A.B., Yao, H.F., Bartmess, J.E.: Ionization mechanism of negative ion-direct analysis in real time: a comparative study with negative ion-atmospheric pressure photoionization. J. Am. Soc. Mass Spectrom. **20**, 42–50 (2009)
17. Nilles, J.M., Connell, T.R., Stokes, S.T., Durst, H.D.: Explosives detection using direct analysis in real time (DART) mass spectrometry. Propellants Explos. Pyrotech. **35**, 446–451 (2010)
18. Sisco, E., Dake, J., Bridge, C.: Screening for trace explosives by AccuTOF^{TM}-DART: an in-depth validation study. Forensic Sci. Int. **232**, 160–168 (2013)
19. Song, L.G., Bartmess, J.E.: Liquid chromatography/negative ion atmospheric pressure photoionization mass spectrometry: a highly sensitive method for the analysis of organic explosives. Rapid Commun. Mass Spectrom. **23**, 77–84 (2009)
20. Domin, M.A., Cody, R.B.: Ambient ionization mass spectrometry. Royal Society of Chemistry, Cambridge (2015)
21. Jones, E.G., Harrison, A.G.: A study of penning ionization reactions using a single-source mass spectrometer. Int. J. Mass Spectrom. Ion Phys. **5**, 137–156 (1970)
22. NIST Standard Reference Database Number 69. http://webbook.nist.gov/chemistry/ (accessed August 11, 2017).
23. Song, L.G., Chuah, W.C., Lu, X.Y., Remsen, E., Bartmess, J.E.: Ionization mechanism of positive-ion nitrogen direct analysis in real time. J. Am. Soc. Mass Spectrom. **29**, 640–650 (2018)
24. Cody, R.B.: Observation of molecular ions and analysis of nonpolar compounds with the direct analysis in real time ion source. Anal. Chem. **81**, 1101–1107 (2009)
25. Song, L.G., Gibson, S.C., Bhandari, D., Cook, K.D., Bartmess, J.E.: Ionization mechanism of positive-ion direct analysis in real time: a transient microenvironment concept. Anal. Chem. **81**, 10080–10088 (2009)
26. Dane, A.J., Cody, R.B.: Selective ionization of melamine in powdered milk by using argon direct analysis in real time (DART) mass spectrometry. Analyst. **135**, 696–699 (2010)
27. Cody, R.B., Dane, A.J.: Dopant-assisted direct analysis in real time mass spectrometry with argon gas. Rapid Commun. Mass Spectrom. **30**, 1181–1189 (2016)
28. Yang, H.M., Wan, D.B., Song, F.R., Liu, Z.Q., Liu, S.Y.: Argon direct analysis in real time mass spectrometry in conjunction with makeup solvents: a method for analysis of labile compounds. Anal. Chem. **85**, 1305–1309 (2013)
29. Borges, D.L.G., Sturgeon, R.E., Welz, B., Curtius, A.J., Mester, Z.: Ambient mass spectrometric detection of organometallic compounds using direct analysis in real time. Anal. Chem. **81**, 9834–9839 (2009)
30. Keelor, J.D., Dwivedi, P., Fernández, F.M.: An effective approach for coupling direct analysis in real time with atmospheric pressure drift tube ion mobility spectrometry. J. Am. Soc. Mass Spectrom. **25**, 1538–1548 (2014)
31. Dwivedi, P., Gazda, D.B., Keelor, J.D., Limero, T.F., Wallace, W.T., Macatangay, A.V., Fernández, F.M.: Electro-thermal vaporization direct analysis in real time-mass spectrometry for water contaminant analysis during space missions. Anal. Chem. **85**, 9898–9906 (2013)
32. Harris, G.A., Kwasnik, M., Fernández, F.M.: Direct analysis in real time coupled to multiplexed drift tube ion mobility spectrometry for detecting toxic chemicals. Anal. Chem. **83**, 1908–1915 (2011)
33. Nah, T., Chan, M.N., Leone, S.R., Wilson, K.R.: Real time in situ chemical characterization of submicrometer organic particles using direct analysis in real time-mass spectrometry. Anal. Chem. **85**, 2087–2095 (2013)
34. Jorabchi, K., Hanold, K., Syage, J.: Ambient analysis by thermal desorption atmospheric pressure photoionization. Anal. Bioanal. Chem. **405**, 7011–7018 (2013)
35. Shi, X.Y., Su, R., Yang, H.M., Lian, W.H., Wan, X.L., Liu, S.Y.: Detection of pharmaceuticals by nitrogen direct analysis in real time mass spectrometry. Chem. J. Chin. Univ.-Chin. **38**, 362–368 (2017)
36. Schmidt, A.C., Herzschuh, R., Matysik, F.M., Engewald, W.: Investigation of the ionisation and fragmentation behaviour of different nitroaromatic compounds occurring as polar metabolites of explosives using electrospray ionisation tandem mass spectrometry. Rapid Commun. Mass Spectrom. **20**, 2293–2302 (2006)
37. Ayoub, K., Nélieu, S., Hullebusch, E.D., Maia-Grondard, A., Cassir, M., Bermond, A.: TNT oxidation by fenton reaction: reagent ratio effect on kinetics and early stage degradation pathways. Chem. Eng. J. **173**, 309–317 (2011)
38. He, X., Zeng, Q., Zhou, Y., Zeng, Q.X., Wei, X.F., Zhang, C.Y.: A DFT study toward the reaction mechanisms of TNT with hydroxyl radicals for advanced oxidation processes. J. Phys. Chem. A. **120**, 3747–3753 (2016)
39. Zhang, J.L., Zhou, Z.G., Yang, J.W., Zhang, W., Bai, Y., Liu, H.W.: Thin layer chromatography/plasma assisted multiwavelength laser desorption ionization mass spectrometry for facile separation and selective identification of low molecular weight compounds. Anal. Chem. **84**, 1496–1503 (2012)
40. Zhao, Q., Liu, J.L., Wang, B., Zhang, X.H., Huang, G.Y., Xu, W.: Rapid screening of explosives in ambient environment by aerodynamic assisted thermo desorption mass spectrometry. J. Mass Spectrom. **52**, 1–6 (2017)
41. Sisco, E., Forbes, T.P., Staymates, M.E., Gillen, G.: Rapid analysis of trace drugs and metabolites using a thermal desorption DART-MS configuration. Anal. Methods. **8**, 6494–6499 (2016)
42. Park, E.J., Kim, H.J., Han, S.W., Jeong, J.H., Kim, H., Seo, H.O., Kim, Y.D.: Assembly of PDMS/SiO_2-PTFE and activated carbon fibre as a liquid water-resistant gas sorbent structure. Chem. Eng. J. **325**, 433–441 (2017)
43. Fu, Y.F., Teng, Y., Yu, G.M., Yin, C.Y.: Synthesis and structure properties of flame retardant and cationic dyeable polyamide 6 modified with 5-sulfoisophthalic acid sodium and melamine cyanurate. Fibers Polym. **19**, 1363–1372 (2018)
44. Tang, C.Y.Y., Kwon, Y.N., Leckie, J.O.: Effect of membrane chemistry and coating layer on physiochemical properties of thin film composite polyamide RO and NF membranes I. FTIR and XPS characterization of polyamide and coating layer chemistry. Desalination. **242**, 149–167 (2009)
45. He, Q.H., Ma, C.C., Hu, X.Q., Chen, H.W.: Method for fabrication of paper-based microfluidic devices by alkylsilane self-assembling and UV/O_3-patterning. Anal. Chem. **85**, 1327–1331 (2013)
46. Jiao, L., Ma, J.X., Dai, H.Q.: Preparation and characterization of self-reinforced antibacterial and oil-resistant paper using a NaOH/Urea/ZnO solution. PLoS One. 1–16 (2015)